Available online at www.sciencedirect.com
ScienceDirect
Chinese Journal of Natural Medicines 2019, **17**(1): 0015–0021
Chinese Journal of Natural Medicines

•Special topic•

Protein tyrosine phosphatase 1B inhibitory activities of ursane-type triterpenes from Chinese raspberry, fruits of *Rubus chingii*

ZHANG Xiang-Yu [1, 3], LI Wei [1, 2*], WANG Jian [1, 3*], LI Ning [1], CHENG Mao-Sheng [1, 3], KOIKE Kazuo [2]

[1] *Key Laboratory of Structure-Based Drug Design & Discovery, Ministry of Education, Shenyang Pharmaceutical University, Shenyang 110016, China;*
[2] *Faculty of Pharmaceutical Sciences, Toho University, Chiba 274-8510, Japan;*
[3] *School of Pharmaceutical Engineering, Shenyang Pharmaceutical University, Shenyang 110016, China*

Available online 20 Jan., 2019

[ABSTRACT] Protein tyrosine phosphatase 1B (PTP1B) has led to an intense interest in developing its inhibitors as anti-diabetes, anti-obesity and anti-cancer agents. The fruits of *Rubus chingii* (Chinese raspberry) were used as a kind of dietary traditional Chinese medicine. The methanolic extract of *R. chingii* fruits exhibited significant PTP1B inhibitory activity. Further bioactivity-guided fractionation resulted in the isolation of three PTP1B inhibitory ursane-type triterpenes: ursolic acid (**1**), 2-oxopomolic acid (**2**), and 2α, 19α-dihydroxy-3-oxo-urs-12-en-28-oic acid (**3**). Kinetics analyses revealed that **1** was a non-competitive PTP1B inhibitor, and **2** and **3** were mixed type PTP1B inhibitors. Compounds **1**−**3** and structurally related triterpenes (**4**−**8**) were further analyzed the structure-activity relationship, and were evaluated the inhibitory selectivity against four homologous protein tyrosine phosphatases (TCPTP, VHR, SHP-1 and SHP-2). Molecular docking simulations were also carried out, and the result indicated that **1**, 3-acetoxy-urs-12-ene-28-oic acid (**5**), and pomolic acid-3*β*-acetate (**6**) bound at the allosteric site including α3, α6, and α7 helix of PTP1B.

[KEY WORDS] Protein tyrosine phosphatase 1B; Raspberry; *Rubus chingii*; Triterpene; Ursane

[CLC Number] R284.3 **[Document code]** A **[Article ID]** 2095-6975(2019)01-0015-07

Introduction

Protein tyrosine phosphatase 1B (PTP1B) is a non-transmembrane protein tyrosine phosphatase, that is expressed ubiquitously in the classical insulin-targeted tissues, and plays critical roles in negatively regulating both insulin and leptin signaling cascades [1-2]. Previous studies demonstrated that PTP1B knockout mice exhibited increased insulin sensitivity and obesity resistance and also played a positive role in tumorigenesis of breast cancer and colorectal cancer [1-2]. These findings have led to an intense interest in developing PTP1B inhibitors as anti-diabetes, anti-obesity and anti-cancer agents [5-6]. Despite several PTP1B inhibitors, such as ertiprotafib and trodusquemine, have been developed into clinical trials, it is still a long way to goal in clinical application [7-8]. Therefore, the use of natural medicines with excellent PTP1B inhibitory activity is a considerable shortcut [9].

Rubus chingii Hu (Rosaceae), a kind of Chinese raspberry, is a perennial woody plant, which is widely distributed in southeast China. The dried immature fruits, referred to as "Fupenzi" in Chinese, have been used as a kind of dietary traditional Chinese medicine, with the function of nourishing kidney and improving the function of urine control. Previous biological investigations have reported cardiovascular, anti-inflammatory and anti-ageing effects [10-12]. Triterpenoids, diterpenoids and flavonoids have been reported as the bioactive constituents [11, 13-14].

During our ongoing investigation to discover novel PTP1B inhibitors from natural resources [15-19], a library consisted of two hundred of extracts from traditional Chinese medicines was screened PTP1B inhibitory activity. As the result, the

[Received on] 20-Aug.-2018
[Research funding] This work was supported by the National Natural Science Foundation of China (No. 81628012).
[*Corresponding author] E-mails: liwei@phar.toho-u.ac.jp (LI Wei); jianwang@syphu.edu.cn (WANG Jian)
These authors have no conflicts of interest to declare.

methanolic extract of *R. chingii* fruits exhibited significant PTP1B inhibitory activity with the IC_{50} of 10.4 μg·mL^{-1}. Therefore, this extract was selected to further investigate the bioactive compounds with PTP1B inhibitory activities.

Results and discussion

The MeOH extract of *R. chingii* fruits was partitioned between EtOAc and H_2O. Since the EtOAc fraction showed PTP1B inhibitory activity, it was carried out further bioactivity-guided fractionation, and resulted in the isolation of three ursane-type triterpenes, namely, ursolic acid (**1**), 2-oxopomolic acid (**2**), and 2α,19α-dihydroxy-3-oxo-urs-12-en-28-oic acid (**3**). The structures were determined by detailed NMR and MS spectroscopic analyses and comparison with literature data [20-22].

Triterpenes **1**–**3** were evaluated PTP1B inhibitory activities at different concentrations. As a result, **1**–**3** inhibited PTP1B in a concentration dependent manner, and the IC_{50} were determined by regression analyses (Table 1). The inhibition modes of compounds **1**–**3** were further elucidated by kinetics analyses with various concentrations of the compounds and the substrate *p*-nitrophenyl phosphate (*p*-NPP). As shown in Fig. 2, Lineweaver-Burk plots indicated compounds **1** was a non-competitive PTP1B inhibitors with the K_i of 25.8 μmol·L^{-1}, and compounds **2** and **3** inhibited PTP1B by a mixed mode. The secondary plots of compounds **1** and **2** showed good linear relationship, when they were created by the slopes from the Lineweaver-Burk plots on the y-axis against the concentration on the x-axis. Meanwhile, the secondary plot of compound **3** showed good linear relationship, when plotting $[I]^2$ on the x-axis, suggesting that two molecules of **3** were involved in the inhibition of PTP1B activity.

Table 1 Inhibitory activities, free energy of binding, H-bond interactions, and hydrophobic interactions between triterpenes 1–8 and PTP1B structure (1T4J)

Compound	IC_{50} (μmol·L^{-1}) [a]	Inhibition mode	*Ki* (μmol·L^{-1})	Glide score (kcal·mol^{-1})	Hydrogen bonds	Hydrophobic interactions
1	7.1 ± 1.0	Non-competitive	25.8	–4.747	**Asn193**, Glu297	Leu192, phe196, Phe280
2	23.7 ± 2.7	Mixed		–4.595	**Asn193**, Lys197, Trp291	Leu192, phe196, Phe280,
3	52.3 ± 7.2	Mixed		–4.086	**Asn193**, Lys197	Leu192, phe196, Phe280
4	18.7 ± 0.9 [b]			–4.596	**Asn193**	Lys197, Phe280
5	4.8 ± 0.5 [b]			–5.047	**Asn193**, Ser295	Leu192, phe196, Phe280
6	6.1 ± 0.3 [b]			–4.742	**Asn193**, Lys197	Leu192, phe196, Phe280
7	39.0 ± 5.4 [b]			–4.589	**Asn193**	Leu192, phe196, Phe280
8	54.8 ± 5.9 [b]			–4.158	**Asn193**, Lys197	phe196, Phe280

[a] IC_{50} were determined by regression analyses and expressed as mean ± SD of three replicates; [b] IC_{50} from reference [23].

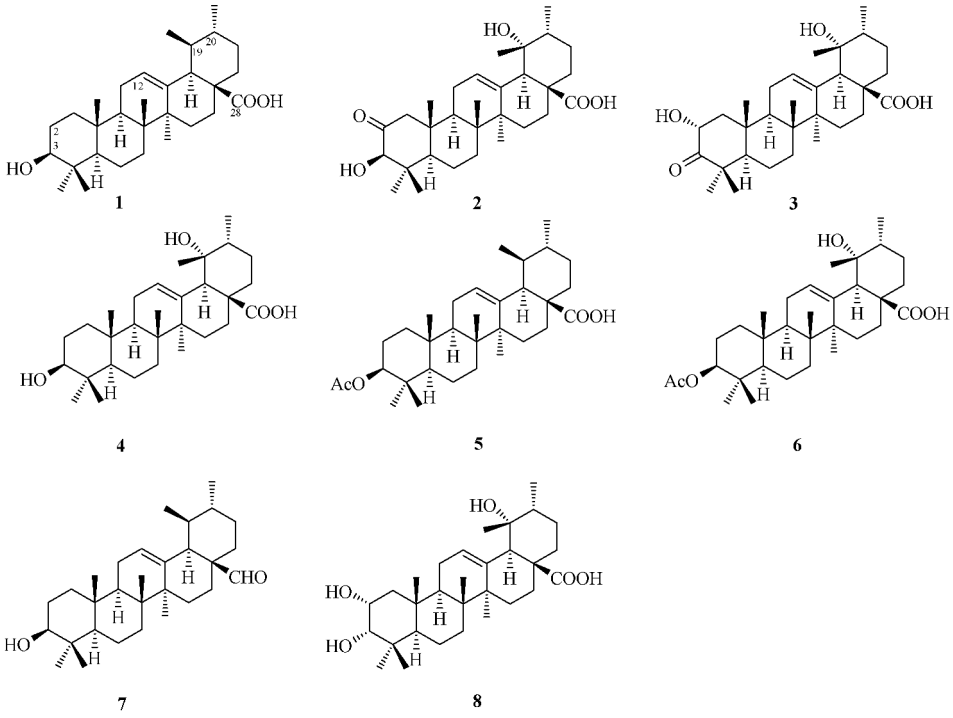

Fig. 1 Chemical structures of triterpenes 1–8

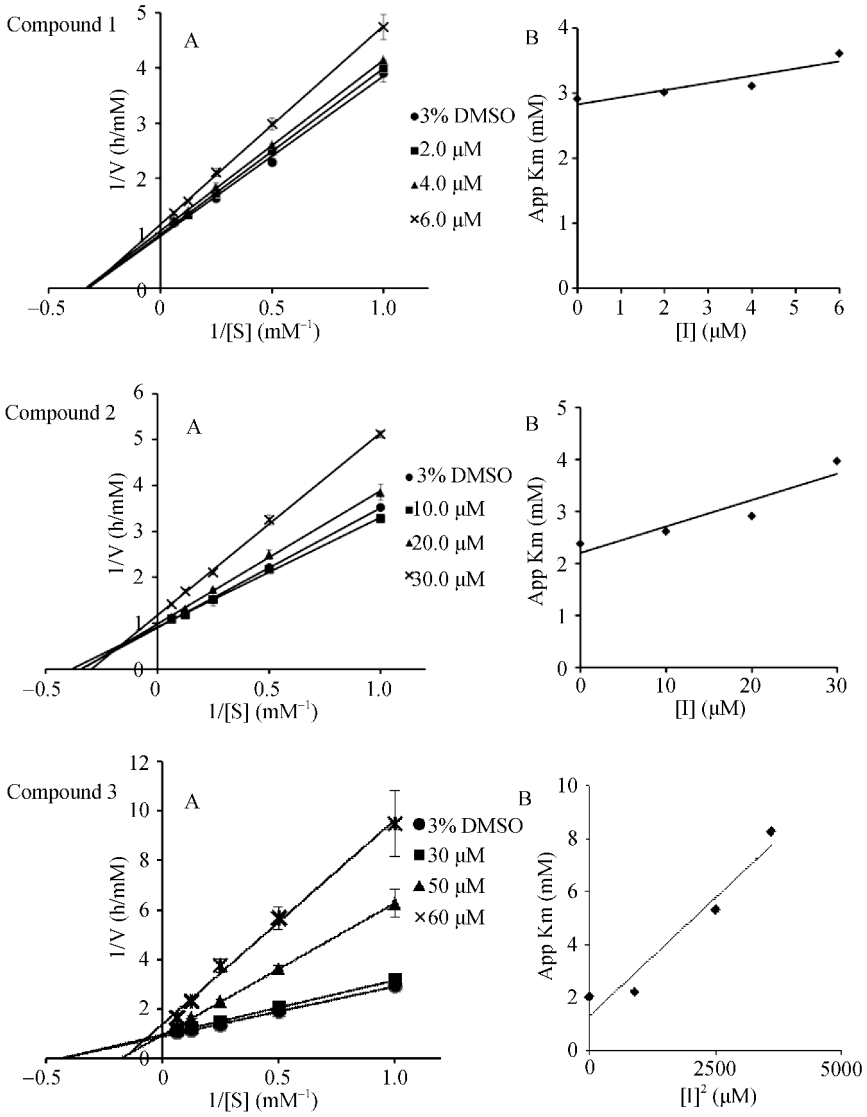

Fig. 2 Inhibition of PTP1B-catalyzed hydrolysis of *p*-NPP by triterpenes 1–3. For each compound, A (left) represents the Lineweaver-Burk plots, and B (right) is the secondary plots from A

To better understand the structure-activity relationship, structurally related ursane-type triterpenes (**4**−**8**), which were previously isolated from *Sorbus pohuashanensis* were selected for comparison [23]. Compounds **1**, **5** and **6**, which showed the most potent PTP1B inhibitory activities, have a common structure of urs-12-en-28-oic acid. Further comparison suggested that 28-carboxy group increased the activity than formyl group (**1** *vs* **7**); acetylation of 3-hydroxy group increase the activity (**1** *vs* **5**; **4** *vs* **6**); 19-hydroxylation decreased the activity (**1** *vs* **4**; **5** *vs* **6**). In comparison to 3-droxylation, more oxidation in A ring decreased the activity (**2**, **3**, **8** *vs* **4**, **6**)

Molecular docking simulation by Glide SP mode was also performed to understand PTP1B inhibition mode of the ursane-type triterpenes. On the basis of aforementioned kinetics analyses, the allosteric site of PTP1B was selected for binding simulation. Since the crystal structures of PTP1B (PDB code 1T4J and 1T48) missed the key residues of α7 helix, the full structure of PTP1B (residues 1−298，including α7 helix) was built and optimized by the softwares DS 3.0 and Desmond 3.7 to improve the accuracy of docking.

The docking results were evaluated by comparing binding energy and docking poses *via* Glide SP mode. Analysis of these results of native docking simulations showed, most binding energy scores could accurately forecast the ligand activities. As shown in the Table 1, the binding energy of compound **1** (IC_{50} 7.1 ± 1.0 μmol·L^{-1}), **5** (IC_{50} 4.8 ± 0.5 μmol·L^{-1}) and **6** (IC_{50} 6.1 ± 0.3 μmol·L^{-1}) were –4.747, –5.047 and –4.742 kcal·mol^{-1}, respectively, which showed the most potent PTP1B inhibitory activities.

The preferred binding patterns of compounds **1**, **5** and **6** within the allosteric site of PTP1B were shown in Fig. 3, and the 2D diagram of the interaction of compounds **1**–**8** was shown in the Fig. 4. As for compound **1,** the 3-hydroxy group donated an H-bond to Glu297 (1.87 Å) in α7 helix, and the

28-carboxy group involved in a strong hydrogen bond formation with Asn193 (1.73 Å, α3 helix). Meanwhile, the E ring formed hydrophobic interactions with Phe196, Leu192, and Phe280. In the case of compound **6**, the 19-hydroxy group formed an H-bond with Lys197 (2.06 Å) and the ester made hydrogen bonds with Asn193 (2.34 Å). The interactions of compound **5** was similar to **1,** however, acetylation of 3-hydroxy group formed an additional carbon H-bond with Ser295 (3.41 Å, α7 helix). In our hypothesis, the acetylation of 3-hydroxy group could occupy an adaptable binding site and stabilize the ligand-protein complexes conformation that improved the activities of compound **5** and **6.**

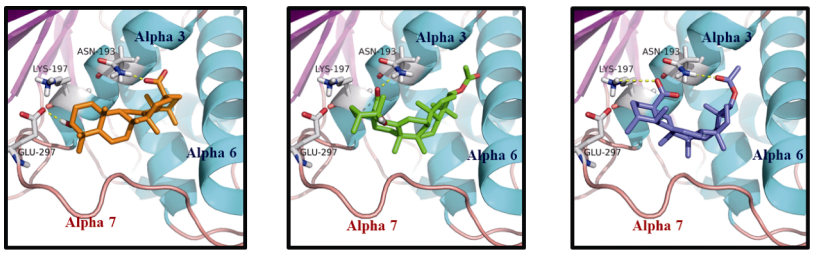

Fig. 3 Docked poses of triterpenes 1 (A, orange stick), 5 (C, green stick) and 6 (B, blue stick) in the allosteric site of PTP1B (including alpha 7 helix). Protein: carbon atoms of key residues (white), nitrogen (blue) and oxygen (red)

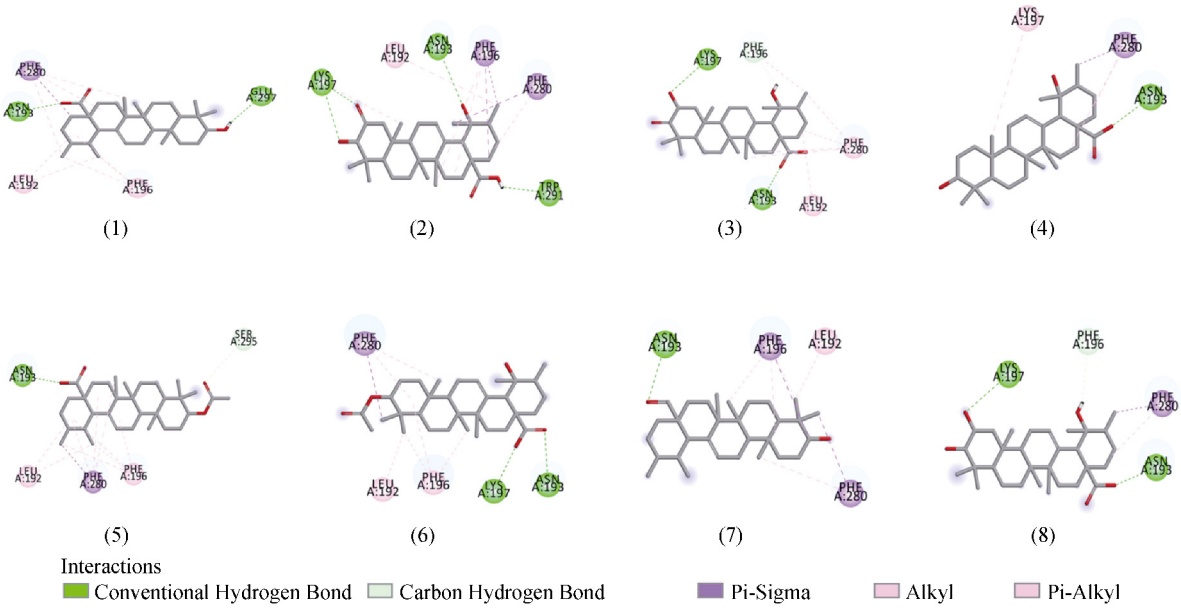

Fig. 4 2D diagram of the interaction of compounds 1–8 in the allosteric site of the PTP1B. Hydrogen bond interactions were shown as green dashed lines, carbon–hydrogen bond interactions were shown as thin green dashed lines, pi–sigma interaction was shown as purple dashed line, alkyl and pi–alkyl interaction was shown as thin pink dashed line

Furthermore, compounds **2** (IC_{50} 23.7 ± 2.7 μmol·L^{-1}) and **4** (IC_{50} 18.7 ± 0.9 μmol·L^{-1}) showed moderate PTP1B inhibitory activities (IC_{50} < 30 μmol·L^{-1}), with similar binding energy (−4.595 and −4.596 kcal·mol^{-1}). The interaction of compound **2** with allosteric site of PTP1B showed the presence of four hydrogen bonds. Analysis of the distance profile showed the formation of H-bonds by 3-hydroxy group and 2-carbonyl group with Lys 197, 19-hydroxy group with Asn193 and 28-carboxy group with Trp291 to be maintained below 3.0 Å. In the meantime, the methyls of D and E rings formed hydrophobic interactions with Leu192, Phe196 and Phe280. Whereas, the compound **4** formed only one H-bond between 28-carboxy group and Asn193 (1.7 Å). Due to rigidity of the ursane-type triterpenes core, both compounds **2** and **4** could not fill the pocket deeper compared with compounds **5** and **6**, which leaded to lower activities.

The binding energy of compounds **3**, **7** and **8** for the docking experiment was calculated to be −4.086,−4.589 and −4.158 kcal·mol^{-1}, respectively. The activities of these compounds are weaker than others. Through analysis of docking poses, we could know that the compound **3** formed H-bond between the 2-hydroxy group and 28-carboxy group with Lys197 and Asn193, respectively, without any residues of α7 helix. And the 28-aldehyde group of compound **7** formed H-bond to Asn193. The interaction of it could be weaker than 28-carboxy group of others. As for compound **8**, 2-OH

formed an H-bond with the main chain of Lys197, and an additional H-bond was formed between Asn193 and the 28-COOH group. Moreover, E ring of compound **8** filled the hydrophobic pocket via Phe280. Unfortunately, compunds **7** and **8** are not formed any interaction with key residues of α7 helix. It can explain that compounds **1**, **5** and **6** showed the most potent PTP1B activities.

Because of the high structural similarity of the catalytic center among the family of protein tyrosine phosphatases (PTPs) [24], the inhibitory selectivity against PTPs is an important factor for development of PTP1B inhibitors. The inhibitory selectivity of compounds **1**–**8** were evaluated by comparison of their inhibitory activity against PTP1B and four homologous PTPs, namely, T-cell protein tyrosine phosphatase (TCPTP), Vaccinia H1-related phosphatase (VHR), and Src homology domain 2-containing protein tyrosine phosphatases 1 and 2 (SHP-1 and SHP-2). As shown in Table 2, compounds **5** and **6** showed similar profile against PTPs. Namely, at a concentration completely inhibited PTP1B, they moderately inhibited SHP-2 and weakly inhibited TCPTP, VHR and SHP-1. However, compound **1** was potent inhibitors of not only PTP1B, but also TCPTP and SHP-2. Compounds **2** and **4**, which showed moderate PTP1B inhibitory activities, had good PTPs selectivity.

In conclusion, the methanolic extract of *R. chingii* fruits showed significant PTP1B inhibitory activity, and three ursane-type triterpenes were identified as the bioactive compounds responsible for the activity. Ursolic acid (**1**) was a previous reported PTP1B inhibitor [20], which is in good agreement with our results. 2-Oxopomolic acid (**2**) and 2α, 19α-dihydroxy-3-oxo-urs-12-en-28-oic acid (**3**) were firstly reported their PTP1B inhibitory activity. Further cellular and *in vivo* based mechanistic investigations would benefit understanding and development of ursane-type triterpenes as natural PTP1B inhibitors.

Table 2 Inhibition rate (%) and selective index of triterpenes 1–8 against PTP1B, TCPTP, VHR, SHP-1, and SHP-2

PTPs	**1**		**2**	
	Inhibition rate (%) [a]	S.I. [b]	Inhibition rate (%) [a]	S.I. [b]
PTP1B	98.6 ± 0.1		97.2 ± 0.4	
TCPTP	96.2 ± 1.3	1.0	28.4 ± 2.6	3.4
VHR	55.0 ± 1.7	1.8	66.5 ± 1.8	1.5
SHP-1	72.6 ± 1.7	1.4	45.7 ± 0.8	2.1
SHP-2	93.1 ± 0.8	1.1	24.3 ± 0.9	4.0
PTPs	**3**		**4**	
	Inhibition rate (%) [a]	S.I. [b]	Inhibition rate (%) [a]	S.I. [b]
PTP1B	96.1 ± 0.6		91.0 ± 0.3	
TCPTP	18.9 ± 1.2	5.1	45.2 ± 1.2	2.0
VHR	58.7 ± 0.9	1.6	22.4 ± 0.9	4.1
SHP-1	39.2 ± 1.0	2.5	16.4 ± 2.3	5.5
SHP-2	26.7 ± 2.7	3.6	25.0 ± 2.2	3.6
PTPs	**5**		**6**	
	Inhibition rate (%) [a]	S.I. [b]	Inhibition rate (%) [a]	S.I. [b]
PTP1B	89.5 ± 1.1		96.7 ± 0.4	
TCPTP	18.0 ± 1.7	5.0	24.4 ± 1.2	4.0
VHR	45.3 ± 0.9	2.0	13.3 ± 1.0	7.3
SHP-1	40.4 ± 0.6	2.2	48.6 ± 1.5	2.0
SHP-2	76.5 ± 2.0	1.2	66.0 ± 1.5	1.5
PTPs	**7**		**8**	
	Inhibition rate (%) [a]	S.I. [b]	Inhibition rate (%) [a]	S.I. [b]
PTP1B	71.2 ± 6.5		70.4 ± 1.5	
TCPTP	18.5 ± 1.6	3.8	46.5 ± 3.8	1.5
VHR	47.4 ± 1.0	1.5	36.4 ± 2.5	1.9
SHP-1	26.6 ± 1.9	2.7	22.8 ± 2.9	3.1
SHP-2	51.4 ± 0.6	1.4	50.5 ± 1.8	1.4

[a] Inhibition rate (%) are mean ± SD from three separate experiments;
[b] S.I.: selective index value (Inhibition rate (%) against PTP1B/Inhibition rate (%) against other PTPs).

Materials and Methods

Instruments and chemicals

The ^{1}H and ^{13}C NMR spectra were measured on a JEOL ECP-500 spectrometer with TMS as the internal reference, and the chemical shifts are expressed in δ (ppm). HR-ESI-TOF-MS was conducted using a JEOL JMS-T100 LP AccuTOF LC-plus mass spectrometer. Diaion HP-20 (Mitsubishi Chemical Corporation, Tokyo, Japan), silica gel (silica gel 60N, Kanto Chemical Co., Inc., Tokyo, Japan) were used for column chromatography. TLC was conducted using Silica gel 60 F254 plates (E. Merck). For preparative HPLC, a JASCO PU-2080 HPLC system, equipped with a JASCO RI-2031 Differential Refractometer detector and a JASCO UV-970 detector, were used. Shisedo CAPSEL-PAK C18 (150 mm × 20 mm i.d.) was used for preparative HPLC.

The absorbance in PTP1B bioassays was measured and recorded on a 2300 EnSpire Multimode Plate Reader (PerkinElmer, Hamburg, Germany). The chemical reagents were as follows. PTP1B (human recombinant), T-cell protein tyrosine phosphatase (TCPTP, human recombinant), and Vaccinia H1-related phosphatase (VHR, human recombinant) were from Enzo Life Sciences, Inc. (Lausen, Switzerland). Src homology domain 2-containing protein tyrosine phosphatases 1 and 2 (SHP-1 and SHP-2, human recombinant), citrate buffer solution (PH 6.0), *para*-nitrophenylphosphate (*p*-NPP), and bovine serum albumin were from Sigma-Aldrich Co., LLC. (St Louis, MO, USA). Sodium chloride (NaCl), dithiothreitol (DTT), and sodium hydroxide (NaOH) were from Wako Pure Chemical Industries, Ltd. (Osaka, Japan), and ethylenediaminetetraacetic acid (EDTA) were from Dojindo Co., Ltd. (Kumamoto, Japan).

Plant materials, extraction and isolation

The unripe fruits of *Rubus chingii* Hu were collected from Heihe city, Heilongjiang Province, China in October 2015, and identified by one of the authors (W.L.). The voucher specimens (TH1504) were deposited at the Department of Pharmacognosy, Faculty of Pharmaceutical Sciences, Toho University, Japan. The dried fruits (1.8 kg) were ultrasonically extracted with MeOH (5L × 3; each 1 h) at room temperature, and evaporated to yield an extract (80 g). The extract was partitioned between EtOAc and H_2O (each 1L × 3), and EtOAc extract (35 g) was chromatographed over a silica gel column with $CHCl_3$−MeOH−H_2O (100 : 0 : 0, 95 : 5 : 0, 9 : 1 : 0, and 6 : 4 : 1) to afford four fractions. The $CHCl_3$ eluting fraction (4g), which showed the most potent PTP1B inhibitory activity, was further separated by repeated silica gel column chromatography and preparative RP-HPLC eluting with 90% MeOH to afford triterpenes **1** (31 mg), **2** (8 mg), and **3** (102 mg). The purities of compounds **1**–**3** were > 98% by HPLC-PDA and ^{1}H NMR spectroscopic analysis.

PTP1B and other PTPs inhibitory activity assay

Protein tyrosine phosphatase activity was measured using *p*-NPP as the substrate. A mixture consisting of *p*-NPP and PTP1B or VHR in a buffer containing 0.06 mol·L^{-1} citrate (PH 6.0), 0.1 mol·L^{-1} NaCl, 1 mmol·L^{-1} ethylenediaminetetraacetic acid, and 1 mmol·L^{-1} dithiothreitol with or without a tested compound solution (prepared in the above buffer solution containing 3% dimethyl sulfoxide), was incubated at 37 °C for 30 min. For TCPTP, SHP-1 and SHP-2, assay buffer (PH 7.0) was prepared using 25 mmol·L^{-1} Tris/HCl, 50 mmol·L^{-1} NaCl, 2 mmol·L^{-1} ethylenediaminetetraacetic acid, 5 mmol·L^{-1} dithiothreitol, 0.01% Brij35 and 1 mg·mL^{-1} bovine serum albumin. The substrate (*p*-NPP) was used at concentrations of 2 mmol·L^{-1} for PTP1B, TCPTP, VHR, and SHP-2 and 16 mmol·L^{-1} for SHP-1. The reaction was terminated by adding 20 μL of 10 mol·L^{-1} NaOH. The reaction mixture was blended by a microplate mixer for 5 min and the amount of produced *p*-nitrophenol was tested by measuring the absorbance at 405 nm (Shimadzu Biospec-mini). The blank was measured in the same way except adding buffer solution instead of the enzyme. The inhibitory activities were further measured at three different concentrations to obtain the IC_{50} by regression analyses. The IC_{50} were obtained by regression analyses with measuring the inhibitory activity at different concentrations. RK-682 was used as a positive control with an IC_{50} of 4.60 ± 0.22 μmol·L^{-1} against PTP1B.

Computational simulation

All computational experiments were conducted on a Dell PowerEdge R900 workstation under RHEL 5.3 platform. Chemical structures were prepared by Sybyl 6.9.1 (Tripos Inc) (Tripos Associates: St. Louis, MO, 2003). The protein structure was prepared in Discovery Studio 3.0 software package (BIOVIA Inc.). Molecular dynamic simulation and docking studies were performed with Desmond 3.7 and standard precision (SP) Glide 9.7, respectively.

Ligand preparation: compounds were sketched and optimized in Sybyl 6.91 with Tripos force field and saved as mol2 format.

Protein preparation: The X-ray crystal structures of PTP1B were downloaded from the RCSB Protein Data Bank: PDB codes 1T4J (residues 1–283) and 1T48 (residues 1–283, and 290–298) (http: //www.rcsb.org/pdb/). The residues 284–298 were built by Biovia Discovery Studio 3.0 (Accelrys Inc., San Diego, CA) to generate a full PTP1B structure (residues 1–298，including α7 helix), which was submitted into 100 ns molecular dynamic simulation. All other parameters were set as default.

Docking: Receptor grids were generated before docking with the active site determined by the position of the co-crystal ligand. Crystal structures of PTP1B (PDB code: 1T4J) were imported into Glide 9.7, defined as the receptor structure and the location of active site with a box of size 15 Å× 15 Å×15 Å. The OPLS 2005 force field was used for grid generation. The standard precision (SP) was set for docking studies with two crucial residues, Lys120 and Arg221, in constrained binding to get accurate results. All other parameters were maintained as default.

References

[1] Byon CHJ, Kusari BA, Kusari J. Protein-tyrosine phosphatase-1B acts as a negative regulator of insulin signal transduction [J]. *Mol Cell Biochem*, 1998, **182**(1-2): 101-108.

[2] Kennedy BP. Role of protein tyrosine phosphatase-1B in diabetes and obesity [J]. *Biomed Pharmacother*, 1999, **53**(10): 466-470.

[3] Elchebly M, Payette P, Michaliszyn E, *et al*. Increased insulin sensitivity and obesity resistance in mice lacking the protein tyrosine phosphatase-1B gene [J]. *Science*, 1999, **283**(5407): 1544-1548.

[4] Bentires AM, Neel BG. Protein-tyrosine phosphatase 1B is required for HER2/Neu-induced breast cancer [J]. *Cancer Res*, 2007, **67**(6): 2420-2424.

[5] Zhang S, Zhang ZY. PTP1B as a drug target: recent developments in PTP1B inhibitor discovery [J]. *Drug Discov Today*, 2007, **12**(9-10): 373-381.

[6] Yip SC, Saha S, Chernoff J. PTP1B: a double agent in metabolism and oncogenesis [J]. *Trends Biochem Sci*, 2010, **35**(8): 442-449.

[7] Erbe DV, Wang S, Zhang YL, *et al*. Ertiprotafib improves glycemic control and lowers lipids *via* multiple mechanisms [J]. *Mol Pharmacol*, 2005, **67**(1): 69-77.

[8] Lantz KA, Hart SG, Planey SL, *et al*. Inhibition of PTP1B by trodusquemine (MSI-1436) causes fat-specific weight loss in diet-induced obese mice [J]. *Obesity*, 2010, **18**(8): 1516-1523.

[9] Combs AP. Recent advances in the discovery of competitive protein tyrosine phosphatase 1B inhibitors for the treatment of diabetes, obesity, and cancer [J]. *J Med Chem*, 2010, **53**(6): 2333- 2344.

[10] Su XH, Duan R, Sun YY, *et al*. Cardiovascular effects of ethanol extract of *Rubus chingii* Hu (Rosaceae) in rats: an *in vivo* and *in vitro* approach [J]. *J Physiol Pharmacol*, 2014, **65**(3): 417-424.

[11] Zhang TT, Wang M, Yang L, *et al*. Flavonoid glycosides from *Rubus chingii* Hu fruits display anti-inflammatory activity through suppressing MAPKs activation in macrophages [J]. *J Func Foods*, 2015, **18**: 235-243.

[12] Zeng HJ, Liu Z, Wang YP, *et al*. Studies on the anti-aging activity of a glycoprotein isolated from Fupenzi (*Rubus chingii* Hu.) and its regulation on klotho gene expression in mice kidney [J]. *Int J Biol Macromol*, 2018, **119**, 470-476.

[13] Hattori M, Kuo KP, Shu YZ, *et al*. A triterpene from the fruits of *Rubus chingii* [J]. *Phytochemistry*, 1988, **27**(12): 3975-3976.

[14] Zhong R, Guo Q, Zhou G, *et al*. Three new labdane-type diterpene glycosides from fruits of *Rubus chingii* and their cytotoxic activities against five humor cell lines [J]. *Fitoterapia*, 2015, **102**: 23-26.

[15] Onoda T, Li W, Sasaki T, *et al*. Identification and evaluation of magnolol and chrysophanol as the principle protein tyrosine phosphatase-1B inhibitory compounds in a Kampo medicine, Masiningan [J]. *J Ethnopharmacol*, 2016, **186**: 84-90.

[16] Sasaki T, Li W, Higai K, *et al*. Canthinone alkaloids are novel protein tyrosine phosphatase 1B inhibitors [J]. *Bioorg Med Chem Lett*, 2015, **25**(9): 1979-1981.

[17] Sasaki T, Li W, Higai K, *et al*. Protein tyrosine phosphatase 1B inhibitory activity of lavandulyl flavonoids from roots of *Sophora flavescens* [J]. *Planta Med*, 2014, **80**(7): 557-560.

[18] Li W, Li S, Higai K, *et al*. Evaluation of licorice flavonoids as protein tyrosine phosphatase 1B inhibitors [J]. *Bioorg Med Chem Lett*, 2013, **23**(21): 5836-5839.

[19] Sasaki T, Li W, Morimura H, *et al*. Chemical constituents from *Sambucus adnata* and their protein-tyrosine phosphatase 1B inhibitory activities [J]. *Chem Pharm Bull*, 2011, **59**(11): 1396-1399.

[20] Gnoatto SC, Dassonville-Klimpt A, Da Nascimento S, *et al*. Evaluation of ursolic acid isolated from *Ilex paraguariensis* and derivatives on aromatase inhibition [J]. *Eur J Med Chem*, 2008, **43**(9): 1865-1877.

[21] Jia Z, Liu X, Liu Z. Triterpenoids from *Sanguisorba alpine* [J]. *Phytochemistry*, 1992, **32**(2): 155-159.

[22] Taniguchi S, Imayoshi Y, Kobayashi E, *et al*. Production of bioactive triterpenes by *Eriobotrya japonica* calli [J]. *Phytochemistry*, 2002, **59**(3): 315-323.

[23] Li D, Li W, Higai K, *et al*. Protein tyrosine phosphatase 1B inhibitory activities of ursane- and lupane-type triterpenes from *Sorbus pohuashanensis* [J]. *J Nat Med*, 2014, **68**(2): 427-431.

[24] Tabernero L, Aricescu AR, Jones EY, *et al*. Protein tyrosine phosphatases: structure-function relationships [J]. *FEBS J*, 2008, **275**(5): 867-882.

Cite this article: ZHANG Xiang-Yu, LI Wei, WANG Jian, LI Ning, CHENG Mao-Sheng, KOIKE Kazuo. Protein tyrosine phosphatase 1B inhibitory activities of ursane-type triterpenes from Chinese raspberry, fruits of *Rubus chingii* [J]. *Chin J Nat Med,* 2019, **17**(1): 15-21.